



Article

Cytotoxic and Apoptotic Effect of *Rubus chingii* Leaf Extract against Non-Small Cell Lung Carcinoma A549 Cells

El-Sayed Khafagy ^{1,2,*} , Ahmed Al Saqr ¹, Hadil Faris Alotaibi ³  and Amr Selim Abu Lila ^{4,5} 

¹ Department of Pharmaceutics, College of Pharmacy, Prince Sattam bin Abdulaziz University, Al-kharj 11942, Saudi Arabia

² Department of Pharmaceutics and Industrial Pharmacy, Faculty of Pharmacy, Suez Canal University, Ismailia 41522, Egypt

³ Department of Pharmaceutical Sciences, College of Pharmacy, Princess Nourah bint AbdulRahman University, Riyadh 11671, Saudi Arabia

⁴ Department of Pharmaceutics and Industrial Pharmacy, Faculty of Pharmacy, Zagazig University, Zagazig 44519, Egypt

⁵ Department of Pharmaceutics, College of Pharmacy, University of Hail, Hail 81442, Saudi Arabia

* Correspondence: e.khafagy@psau.edu.sa; Tel.: +966-533-564-286

Abstract: *Rubus chingii* is a traditional Chinese medicinal herbal that has been used since ancient times for its great dietary and medicinal values. Recent reports have underscored the promising cytotoxic effect of *R. chingii* extracts against a wide variety of cancer cells. Therefore, in the current study, we aim to explore the anticancer potential of the *Rubus chingii* ethanolic leaf extract (RcL-EtOH) against non-small cell lung cancer A549 cells. RcL-EtOH efficiently exerted a cytotoxic effect against A549 cells in a dose dependent manner, whilst, it exhibited non-significant toxic effects on normal murine macrophage cells, signifying its safety against normal cells. The reduced viability of A549 cells was reaffirmed by the acridine orange/ethidium bromide double staining, which confirmed the induction of apoptosis in RcL-EtOH-treated A549 cells. In addition, RcL-EtOH instigated the dissipation of mitochondrial membrane potential ($\Delta\Psi_m$) with mutual escalation in ROS generation in a dose-dependent manner. Furthermore, RcL-EtOH increased caspase-3, caspase-9 levels in A549 cells post-exposure to RcL-EtOH, which was concomitantly followed by altered mRNA expression of apoptotic (anti-apoptotic: Bcl-2, Bcl_{XL}; pro-apoptotic: Bax, Bad). To sum up, the RcL-EtOH-instigated apoptotic cell death within A549 cells was assumed to be accomplished via targeting mitochondria, triggering increased ROS generation, with subsequent activation of caspase cascade and altering the expression of gene regulating apoptosis. Collectively, RcL-EtOH might represent a plausible therapeutic option for the management of lung cancer.



Citation: Khafagy, E.-S.; Al Saqr, A.; Alotaibi, H.F.; Abu Lila, A.S.

Cytotoxic and Apoptotic Effect of *Rubus chingii* Leaf Extract against Non-Small Cell Lung Carcinoma A549 Cells. *Processes* **2022**, *10*, 1537. <https://doi.org/10.3390/pr10081537>

Academic Editor: Bonglee Kim

Received: 24 July 2022

Accepted: 4 August 2022

Published: 5 August 2022

Publisher's Note: MDPI stays neutral with regard to jurisdictional claims in published maps and institutional affiliations.



Copyright: © 2022 by the authors. Licensee MDPI, Basel, Switzerland. This article is an open access article distributed under the terms and conditions of the Creative Commons Attribution (CC BY) license (<https://creativecommons.org/licenses/by/4.0/>).

Keywords: anti-cancer; apoptosis; mitochondrial membrane potential; reactive oxygen species (ROS); *Rubus chingii*

1. Introduction

Lung cancer is the most commonly occurring cancer among men globally [1]. As per the latest report of Global Cancer Observatory, lung cancer constituted 11.4% (2,206,771) of all the cancer cases (19,292,789) reported during 2020. In addition, lung cancer was responsible for 1,796,144 fatalities, which constituted up to 18% of the all reported fatalities (9,958,133) resulting from different cancer related malignancies during 2020 [2]. These statistics explicitly outline the danger possessed by lung cancer as a threat for global health and economic burden.

Clinically, lung cancer is classified primarily as small-cell (SCLC) and non-small cell lung cancer (NSCLC), respectively, where the latter is responsible for approximately 80% of all the cases of lung cancer [3]. The clinical management of patient with lung cancer is optimally dependent on the stage at which a patient is diagnosed with such dreaded

malignancy, and it usually involves surgical resection, which is simultaneously followed by chemo- and/or radio-therapy [4]. Chemotherapeutic drugs including paclitaxel, 5-fluorouracil (5-FU), docetaxel, cisplatin and gemcitabine are the primarily used therapeutics against lung cancer. However, the development of drug resistance in lung carcinoma has substantially attenuated the efficacy of various chemotherapeutic drugs [5–7]. Moreover, the chemotherapeutic intervention against lung carcinomas usually leads to severe off-target effects. Accordingly, there is a global surge for exploring alternative therapies with better tolerance profile, such as natural products, to replace the commonly used chemotherapeutics.

Historically, plants have served as a source for bioactive phyto-constituents, which exhibit intrinsic therapeutic efficacies against several chronic disorders, including cancers. Such therapeutic efficiencies of plants are entirely related to an array of secondary metabolites including lignans, quinones, flavonoids, and terpenoids, among others [8,9]. Currently, cancer chemoprevention with natural herbal constituents and phytochemical compounds is considered as a promising strategy to prevent, delay, impede, or cure cancer. It is estimated that 50–60% of cancer patients in the United States use medications derived from plants exclusively or concomitantly with conventional therapeutic regimens such as chemo- and/or radio-therapy [10].

Rubus chingii Hu (*R. chingii*), Chinese immature raspberry, has had great dietary and medicinal values since the ancient times. *R. chingii* was identified to contain abundant bioactive components, including flavonoids, diterpenoids, triterpenoids, and organic acids [11]. Owing to these bioactive components, *R. chingii* was recognized to have diverse pharmacological activities such as antimicrobial, anti-aging and anti-inflammatory activities [11,12]. In addition, recent preclinical explorations have substantially indicated the anti-cancer potential of *R. chingii* against various types of cancers [13–16]. The aim of the current study, therefore, was to explore the anti-cancer effect of *R. chingii* ethanolic leaf extract (RcL-EtOH) against NSCLC A549 cells. The results of this study emphasized that RcL-EtOH exerted its cytotoxic potential against A549 via prompting reactive oxygen species (ROS)-dependent mitochondria-mediated intrinsic apoptosis as evidenced by dissipation of mitochondrial membrane potential ($\Delta\Psi_m$), bax/bcl-2 dysregulation, and activation of caspases 3 and 9.

2. Materials and Methods

2.1. Materials

5-Fluorouracil (5-FU), 3-(4,5-dimethylthiazol-2-yl)-2,5-diphenyl tetrazolium bromide (MTT), 2,7-dichlorodihydrofluorescein diacetate (DCFH-DA), ethidium bromide (EtBr), acridine orange (AO), rhodamine-123 (Rh-123), Caspase-3 (CASP3C-1KT), and Caspase-9 (APT 173) kits were obtained from Sigma Aldrich (St. Louis, MO, USA). Dulbecco's modified Eagle medium (DMEM), fetal bovine serum (FBS) and antibiotic-antimycotic solution were purchased from Gibco (Gaithersburg, MD, USA) whereas the colorimetric kit specific for caspase-9 and -3 was procured from BioVision, USA. The cDNA synthesis kit (Verso) was supplied by Thermo-Scientific (Waltham, MA, USA). Integrated DNA Technologies (IDT, Coralville, IA, USA) provided all the primers used in this study.

2.2. Plant Material

The leaves of *Rubus chingii* plants were collected from different forest/rural areas in the Gulmi district of central Nepal. The collected *R. chingii* plant was assigned different batches; namely A, B, and C, which were subsequently authenticated by an expert botanist and submitted to the institutional herbarium of Integral University with a voucher number: IU/PHAR/HRBD/22/05.

2.3. Preparation of Ethanolic Leaf Extract

The leaves of *R. chingii* from different batches were cleaned using running tap water and were left for drying in the shed for approximately a week. The leaves were then powdered using pestle and mortar. Subsequently, the powdered leaves from different

batches underwent extraction using a Soxhlet apparatus for 5 h in ethanol (60–65 °C). The obtained leaf extract from different batches was further subjected to two rounds of filtration via Whatman No. 1 paper filters. The leftover solvent was air-dried for a couple days at room temperature to yield a dried sticky extract of *R. chingii* leaves (RcL-EtOH), which was kept at 4 °C until subsequent use.

2.4. In Vitro Anti-Cancer Efficacy of RcL-EtOH

2.4.1. Cell Lines

Human non-small cell lung cancer A549 cells (CRM-CCL-185™) and murine macrophage J774A.1 cells (TIB-67™) were provided from American Type Culture Collection (ATCC, Boston, MA, USA). The cells were maintained in DMEM enriched with FBS (10% *v/v*) and antibiotic-antimycotic solution (1%). The cells were incubated in a humidified atmosphere of 5% CO₂ at 37 °C.

2.4.2. Cytotoxicity Assay

The cytotoxicity of RcL-EtOH from different batches was evaluated against cancerous A549 and non-cancerous J774A.1 using MTT dye in accordance to the protocol reported earlier [17]. Briefly, A549 and J774A.1 cells were plated onto a 96-well plate, at a density of 1×10^3 cells per well, and incubated overnight for adherence at 37 °C. The cells were then exposed to varying concentrations, ranging from 12.5 to 200 µg/mL, of either a standard cytotoxic agent (5-FU) or RcL-EtOH and further incubated for 48 h prior treatment with MTT reagent. Post definite incubation time, 10 µL of MTT reagent (5 mg/mL) was transferred to each well followed by incubating the plate for 4 h at 37 °C. Finally, 100 µL of DMSO were added to each to solubilize the formed formazan crystals, and then the optical density was recorded at 490 nm using a Bio-Rad microplate reader (Hercules, CA, USA). Based on the absorbance results, the concentration of the test substance resulting in 50% cellular cytotoxicity of cancer cells (IC₅₀) was estimated.

2.5. Assessment of Reactive Oxygen Species (ROS)

ROS levels within A549 cells was assessed following treatment with RcL-EtOH using the fluorescent marker 2,7-dichlorodihydrofluorescein diacetate (DCFH-DA), as previously described [18]. In brief, A549 cells were plated onto a 96-well plate, at a density of 5×10^3 cells per well, and were allowed to incubate overnight for adherence under standard culture conditions. Subsequently, A549 cells were treated with 50, 100 and 200 µg/mL of RcL-EtOH and were further incubated for 48 h. The treated cells were then trypsinized, rinsed and incubated with DCFH-DA (10 µM) in the dark at room temperature for 30 min. The DCF-DA-mediated fluorescence intensity was visualized as green fluorescent in the photomicrographs of RcL-EtOH-treated A549 cells using the FLoid imaging station (Thermo-Scientific, Waltham, MA, USA).

2.6. Estimation of Mitochondrial Membrane Potential ($\Delta\Psi_m$)

The potential of RcL-EtOH for modulating the $\Delta\Psi_m$ of A549 cells was estimated using Rhodamine (Rh)-123 stain, as previously stated [19]. Briefly, A549 cells were plated onto a 96-well plate, at a density of 5×10^3 cells per well, and were allowed to incubate overnight for adherence under standard culture conditions. Subsequently, the cells were exposed to varying concentrations of RcL-EtOH (50, 100 and 200 µg/mL) for 48 h. Post-RcL-EtOH exposure, the cells were subjected to Rh-123 (5 mg/mL) in the dark for 30 min. Green fluorescent photomicrographs of A549 were recorded using the FLoid imaging station.

2.7. Cytochrome-c Release Assay

The cytochrome-c release assay was performed, as described previously [20]. In brief, 1×10^5 A549 cells/well were treated with definite concentrations (50, 100 or 200 µg/mL) of RcL-EtOH and incubated for 48 h. The cells were harvested, rinsed thrice with ice-cold PBS, and then centrifuged for 10 min at 1000 rpm and 4 °C. The total protein content in cells was

extracted by tissue protein extraction reagent (T-PER; Thermo Fischer Scientific, Waltham, MA, USA). An ELISA kit (KHO1051; Thermo Fischer Scientific, Waltham, MA, USA) was then used to quantify the concentration of cytochrome-c within the total extracted protein following the manufacturers' protocol.

2.8. Apoptosis Assay

Dual acridine orange/ethidium bromide (AO/EB) fluorescence staining was utilized to reveal R_cL-EtOH-induced apoptosis in A549 cells [21]. Briefly, A549 cells were plated onto a 96-well plate, with a cell density of 1×10^5 cells/well, and left overnight for adherence under standardized culture conditions. Subsequently, the cells were left untreated or treated with 50, 100, or 200 $\mu\text{g}/\text{mL}$ of R_cL-EtOH for 48 h. After incubation, the cells were trypsinized, rinsed three times with cold phosphate buffer saline and were pelleted through centrifugation for 2 min at 4 °C and 1500 rpm. Dual fluorescent staining solution (1 μL) containing 100 $\mu\text{g}/\text{mL}$ AO and 100 $\mu\text{g}/\text{mL}$ EB was added to each cell suspension for approximately 15 min. Finally, the suspension was visualized and fluorescent photomicrographs were captured through the FLoid imaging station.

2.9. Assessment of Caspase-3, Caspase-9

Caspase-9 and -3 colorimetric assay kits were utilized to evaluate caspase activity in human lung cancer cells. Briefly, 3×10^6 A549 cells were exposed to 50, 100, or 200 $\mu\text{g}/\text{mL}$ of R_cL-EtOH. At 48 h post-incubation, the cells were harvested and rinsed three times with cold phosphate buffer saline by centrifugation for 2 min at 4 °C and 1500 rpm. Cell pellets were re-suspended in 50 μL lysis buffer and left on ice for 10 min. Subsequently, cell lysates were subjected to centrifugation (10,000 rpm at 4 °C) for 1 min. Then, 50 μL of supernatant was added in each well of a 96-well plate and mixed with an equal volume of 10 mM dithiothreitol and 4 mM substrate (DEVD-pNA), and the plate was then incubated for 10 min. Finally, the absorbance of each well was recorded at 405 nm and the observations were expressed as percentage (%) change in caspase activity, compared to untreated cells.

To determine the impact of pretreatment with caspase inhibitor(s) on cell viability, A549 cells were pre-treated with 50 μM of either Z-DEVD-FMK (caspase-3 inhibitor) or Z-LEHD-FMK (caspase-9 inhibitor) for 2 h. The cells were thereafter treated for 48 h with varying concentrations of R_cL-EtOH, as stated above. Finally, cell viability of R_cL-EtOH-treated A549 cells was evaluated through MTT, as previously stated.

2.10. Quantitative RT-PCR

A total of 1×10^5 A549 cells were exposed to 50, 100 and 200 $\mu\text{g}/\text{mL}$ of R_cL-EtOH and were incubated at 37 °C for a specified period. At 48 h post-treatment, total RNA from each treatment group was extracted using commercially available kit following manufacturer instructions. Subsequently, 2 μg RNA was used for synthesizing cDNA using Verso cDNA kit (Thermo-Scientific, Waltham, MA, USA). The primers used in the study are reported in Table 1 [20]. Glyceraldehyde 3-phosphate dehydrogenase (GAPDH) gene was utilized for normalization. The relative CT approach was employed to assess changes in gene expression in relation to the GAPDH gene. The $\Delta\Delta\text{CT}$ method was used to assess the normalized levels of mRNA for each gene.

Table 1. RT-PCR primers list.

Gene	Sequence	
	Forward	Reverse
GAPDH	CGACCACTTTGTC AAGCTCA	CCCCTCTCAAGGGGTCTAC
Bax	GCTGGACATTGGACTTCCTC	CTCAGCCCATCTTCTCCAG
Bad	CCTCAGGCCTATGCAAAAAG	AAACCCAAAACCTCCGATGG
Bcl-2	ATTGGGAAGTTTCAAATCAGC	TGCATTCTTGGACGAGGG
CDK4	CCTGGCCAGAATCTACAGCTA	ACATCTCGAGGCCAGTCATC
p21 ^{Cip1}	TGTCCGTCAGAACCCATG	GTGGGAAGGTAGAGCTTGG
CyclinD1	CTTCCTCTCCAAAATGCCAG	AGAGATGGAAGGGGGAAAGA
Bcl _{XL}	CAGAGCTTTGAACAGGTAG	GCTCTCGGGTGCTGTATTG

2.11. Statistical Evaluation

The data presented in this study reflect the mean \pm SD of three independent experiments. GraphPad Prism (Ver. 5) was used to establish significance among different groups using the Student's *t*-test and one-way ANOVA, followed by Dunnett's post hoc test. A *p* value of <0.05 was considered significant.

3. Results

3.1. R_cL-EtOH Exerted Cytotoxic Effects against A549 Cells

In order to ascertain the anti-cancer efficacy of R_cL-EtOH against A549 cells, MTT assay was conducted post-R_cL-EtOH exposure for 48 h. As depicted in Figure 1A, treatment with R_cL-EtOH (0–200 μ g/mL) induced a dose-dependent reduction in the cellular viability of A549 cells. The viability of A549 cells was reduced from $87.46 \pm 2.29\%$ to $33.73 \pm 3.87\%$ upon increasing R_cL-EtOH concentration from 12.5 to 200 μ g/mL (Figure 1A). The estimated IC₅₀ value of R_cL-EtOH against A549 cells was 99.98 μ g/mL. Interestingly, the cytotoxic potential of different concentrations of R_cL-EtOH against A549 cells was comparable to that of a standard anticancer compound, 5-fluorouracil (5-FU), indicating the anti-cancer efficacy of R_cL-EtOH against A549 cells.

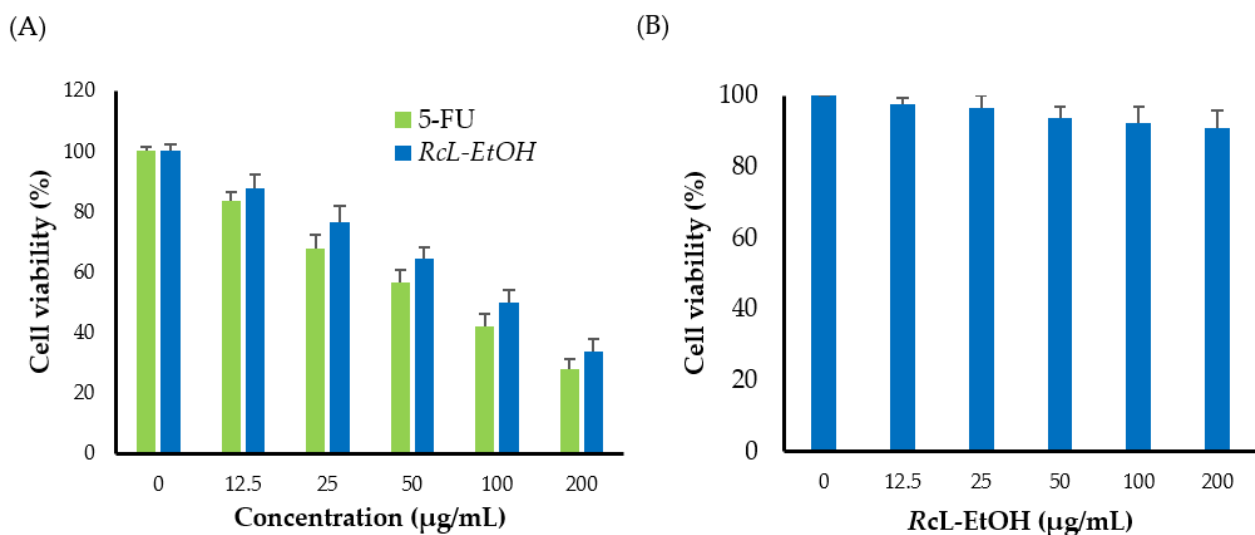


Figure 1. R_cL-EtOH-mediated cytotoxicity in A549 cells. (A) Cell viability percentage of A549 cells post-treatment with either 5-fluorouracil (5-FU), and R_cL-EtOH (0–200 μ g/mL) for 48 h. (B) Cell viability percentage of J774A.1 cells post-treatment with R_cL-EtOH. Data represents mean \pm SD (n = 3).

To address the safety profile of R_cL-EtOH against noncancerous cells, the *in vitro* cytotoxicity of R_cL-EtOH was studied against noncancerous murine J774A.1 cells using

the MTT assay. As demonstrated in Figure 1B, treatment with varying concentrations of RcL-EtOH (0–200 $\mu\text{g}/\text{mL}$) did elicit a significant change in J774A.1 cell viability when compared to that of untreated cells. These findings highlighted the cytotoxic ability of RcL-EtOH against malignant A549 cells but not normal murine J774A.1 cells.

3.2. RcL-EtOH-Induced Apoptosis in A549 Cells

To gain an insight into the possible mechanism of the cytotoxic effect of RcL-EtOH against A549 cells, dual acridine orange/ethidium bromide (AO/EB) staining was performed and fluorescence imaging was adopted to ascertain the viable (VI) and apoptotic (AO) cell numbers. AO/EB staining (Figure 2A) revealed significant cell deaths in cells treated with RcL-EtOH for 48 h, compared to control untreated cells, as manifested by increased red-orange fluorescence in RcL-EtOH-treated cells. In addition, treatment with RcL-EtOH triggered a dose-dependent induction of apoptotic cell death within A549 cells (Figure 2B). The mean percentage of ethidium bromide positive (EB⁺) cells following 48 h treatment with 200 $\mu\text{g}/\text{mL}$ RcL-EtOH ($63.3 \pm 5.6\%$) was much higher than those following treatment with either 100 or 50 $\mu\text{g}/\text{mL}$ RcL-EtOH ($28.2 \pm 3.5\%$ and $48.6 \pm 4.2\%$, respectively). These results suggest that RcL-EtOH-induced cell growth inhibition was, at least in part, a consequence of apoptotic cell death.

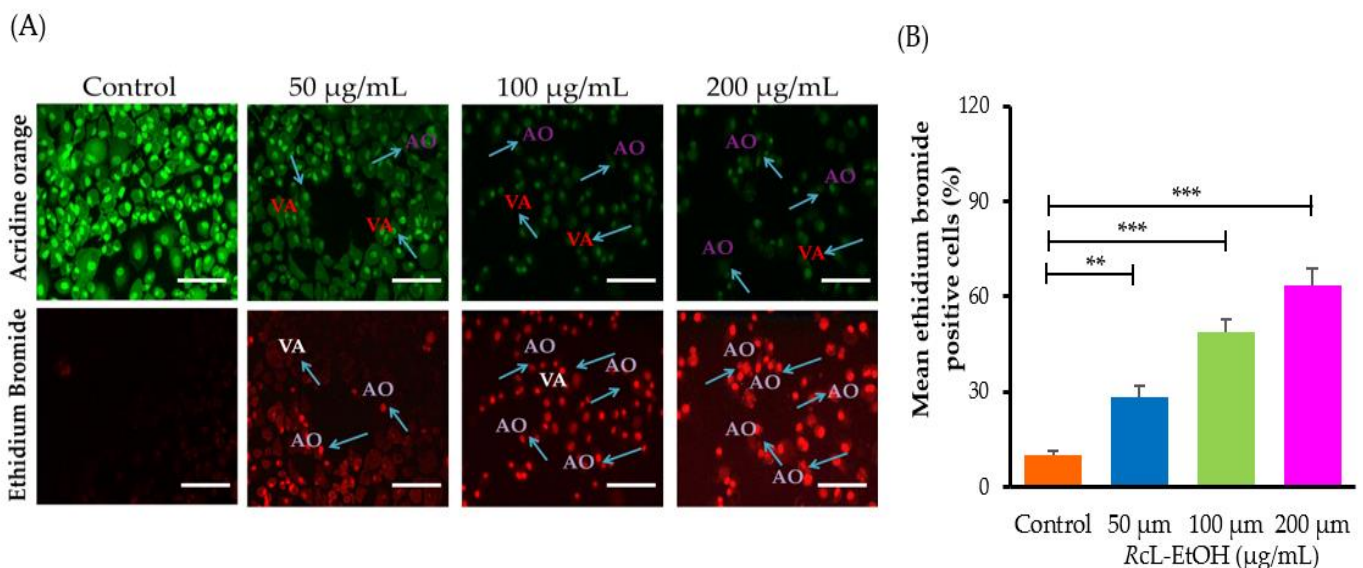


Figure 2. (A) Detection of RcL-EtOH-mediated cell death with acridine orange/ethidium bromide (AO/EB) double staining. Scale bar = 100 μm . (B) Proportion of dead cells (EB⁺ cells). ** $p < 0.01$, *** $p < 0.001$ vs. control.

3.3. RcL-EtOH Exposure Dissipated $\Delta\Psi_m$ and Instigate Mitochondrial Cytochrome-c Release

Mitochondrial membrane potential ($\Delta\Psi_m$) plays a major role in vital mitochondrial functions and its regulation is crucial for cell survival [22]. Disruption in normal mitochondrial functions, specifically alterations in $\Delta\Psi_m$, is considered an early marker of apoptotic cell death [23]. To study the effect of RcL-EtOH on the function of mitochondria, $\Delta\Psi_m$ of A549 cells was evaluated, at 48 h post-treatment with RcL-EtOH, using the mitochondrial voltage-specific reporter rhodamine 123 (Rh 123). Figure 3A revealed that control untreated A549 cells retained an intact $\Delta\Psi_m$, as evidenced by efficient Rh 123 dye cellular uptake and high fluorescence intensity. In contrast, treatment with RcL-EtOH adversely affected the integrity of mitochondrial membrane with a subsequent dissipation of $\Delta\Psi_m$, which was evident by the dose-dependent drop in the uptake of Rh 123 dye by A549 cells (Figure 3B). These findings suggest that the dissipation of $\Delta\Psi_m$ could participate in the RcL-EtOH apoptotic potential against A549 cells.

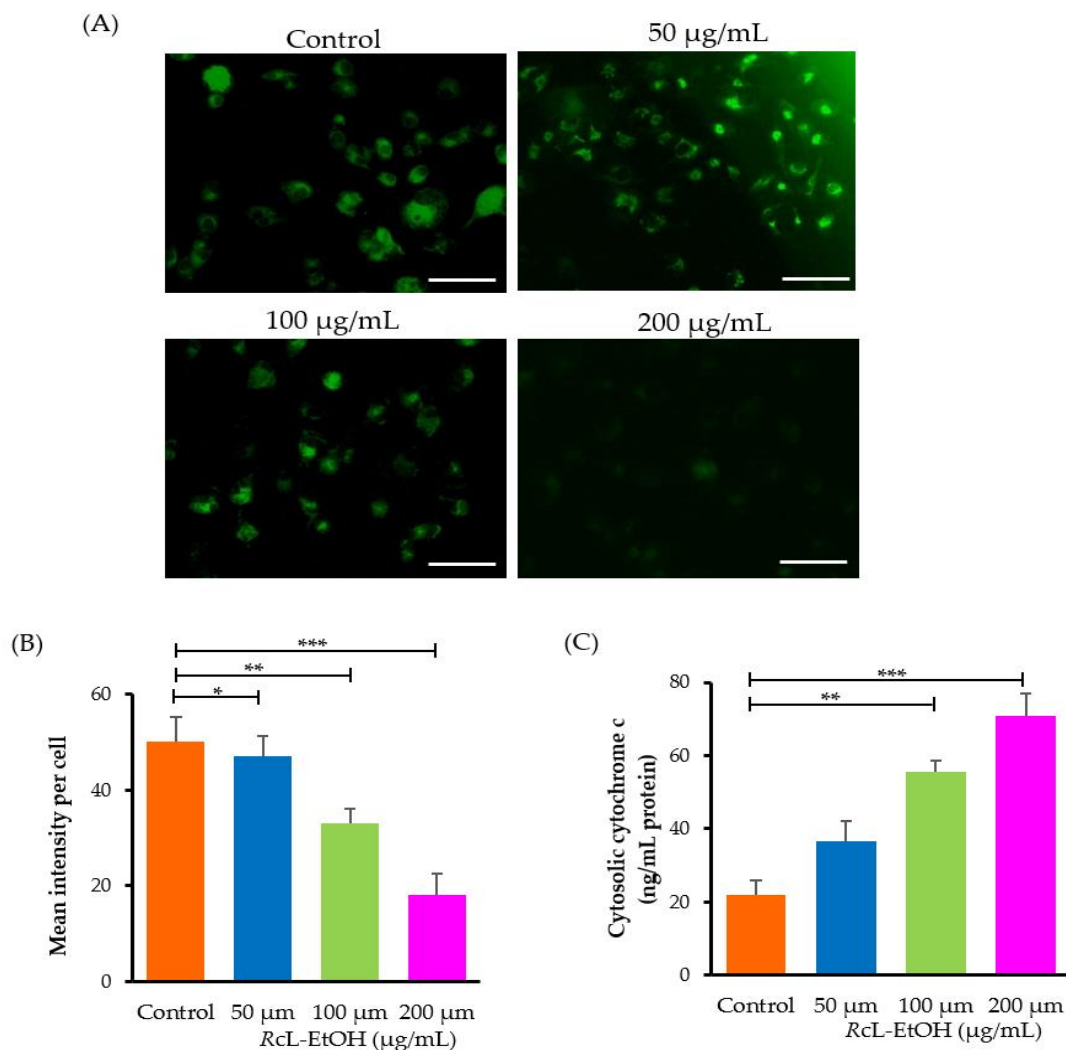


Figure 3. (A) Photomicrographs depicting the dissipation of $\Delta\Psi_m$ within A549 cells post-treatment with varying concentrations (50, 100 and 200 $\mu\text{g}/\text{mL}$) of RcL-EtOH. Scale bar = 100 μm . (B) Quantification of mean fluorescence intensity. (C) Effect of RcL-EtOH on cytosolic cytochrome c. * $p < 0.01$, ** $p < 0.01$, *** $p < 0.001$ vs. control.

Cytochrome c is often released from mitochondria during the early stages of apoptosis [24]. Accordingly, in order to verify the key role of mitochondria in the initiation of apoptosis, the intracellular levels of cytochrome c release were quantified. The results demonstrated in Figure 3C demonstrated that treatment with RcL-EtOH efficiently triggered mitochondrial cytochrome c release in a dose-dependent manner. Treatment with 200 $\mu\text{g}/\text{mL}$ of RcL-EtOH significantly increased the intracellular cytochrome c level by more than 3 folds, compared to untreated control cells. Collectively, these results emphasize the contributing role of mitochondria in the initiation of RcL-EtOH-mediated apoptosis against A549 lung cancer cells.

3.4. Activities of Caspase-3 and Caspase-9 Increased after RcL-EtOH Exposure

Cytochrome c plays a crucial role in the activation of the apoptotic intrinsic pathway via activating the caspase cascade [25]. In addition, activation of the caspase cascade is an important biological marker of apoptosis [26]. Consequently, in order to address whether RcL-EtOH-induced cell death progresses via caspase activation, the activities of caspase-3 and caspase-9 in A549 cells were evaluated post-treatment with RcL-EtOH. The results explicitly revealed that the activity of caspases was increased within A549 cells after treatment with 50, 100 and 200 $\mu\text{g}/\text{mL}$ of RcL-EtOH (Figure 4A). Caspase-3 activity was

enhanced by $67.36 \pm 3.89\%$ (50 $\mu\text{g}/\text{mL}$), $99.79 \pm 4.03\%$ (100 $\mu\text{g}/\text{mL}$) and $127.87 \pm 5.01\%$ (200 $\mu\text{g}/\text{mL}$), whereas that of caspase-9 was found to be $44.98 \pm 3.97\%$ (50 $\mu\text{g}/\text{mL}$), $61.06 \pm 3.49\%$ (100 $\mu\text{g}/\text{mL}$) and $86.25 \pm 5.50\%$ (200 $\mu\text{g}/\text{mL}$) in comparison with the control (Figure 4A). The role of caspases in inducing apoptosis within R_cL-EtOH treated A549 cells was also confirmed through caspase inhibitors. The results demonstrated that caspase-3 (Figure 4B), and -9 (Figure 4C) inhibitors (Z-DEVD-FMK and Z-LEHD-FMK, respectively) considerably ameliorated the cytotoxic effects of R_cL-EtOH against A549 cells. These findings clearly outline the contribution of caspase activation to the instigation of apoptosis within A549 cells post-R_cL-EtOH exposure.

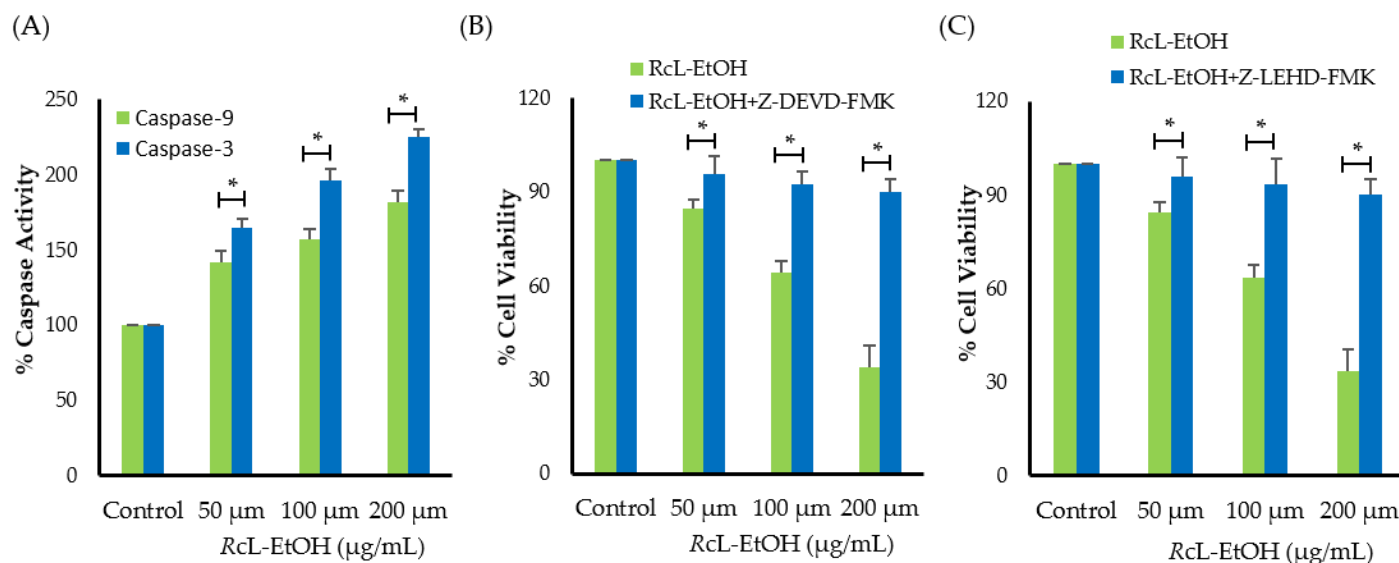


Figure 4. (A) Impact of R_cL-EtOH on caspase-3 and -9 activities. Cell viability of A549 cells pre-treated with inhibitors of (B) caspase-3 and (C) caspase-9. * $p < 0.05$.

3.5. R_cL-EtOH Instigated Intracellular ROS

Reactive oxygen species (ROS) play a vital role in the induction of apoptotic pathways in cancer cells [27]. Consequently, in order to verify whether the apoptotic potential of R_cL-EtOH is mediated via the production of ROS in A549 cells, ROS levels were estimated using the cell permeable dye, DCFH-DA. As shown in Figure 5, treatment with R_cL-EtOH resulted in a dose-dependent aggravation in ROS generation within A549 cells, as manifested with an obvious increase in DCFH-DA-mediated fluorescence compared to control cells (Figure 5A). In the same context, quantitative analysis of DCFH-DA-mediated fluorescence intensity indicated that R_cL-EtOH triggered ROS production in A549 cells in a dose-dependent manner; ROS levels increased from $147.58 \pm 2.8\%$ upon treatment with 50 $\mu\text{g}/\text{mL}$ R_cL-EtOH to $211.45 \pm 4.5\%$ upon treatment with 200 $\mu\text{g}/\text{mL}$ R_cL-EtOH (Figure 5B).

Furthermore, in order to confirm the contribution of ROS production levels to the cytotoxic potential of R_cL-EtOH against A549 cells, A549 cells were pretreated with 10 mM of the antioxidant N-acetyl cysteine (NAC) for 1 h followed by the estimation of cell viability of A549 cells upon treatment with different concentrations of R_cL-EtOH for 48 h. As depicted in Figure S1, the cytotoxic potential of R_cL-EtOH was significantly blocked in A549 pretreated with NAC, presumably via alleviating the production of ROS. These results clearly confirm that the generation of ROS plays a crucial role in the induction of cell death in A549 cells in response to R_cL-EtOH.

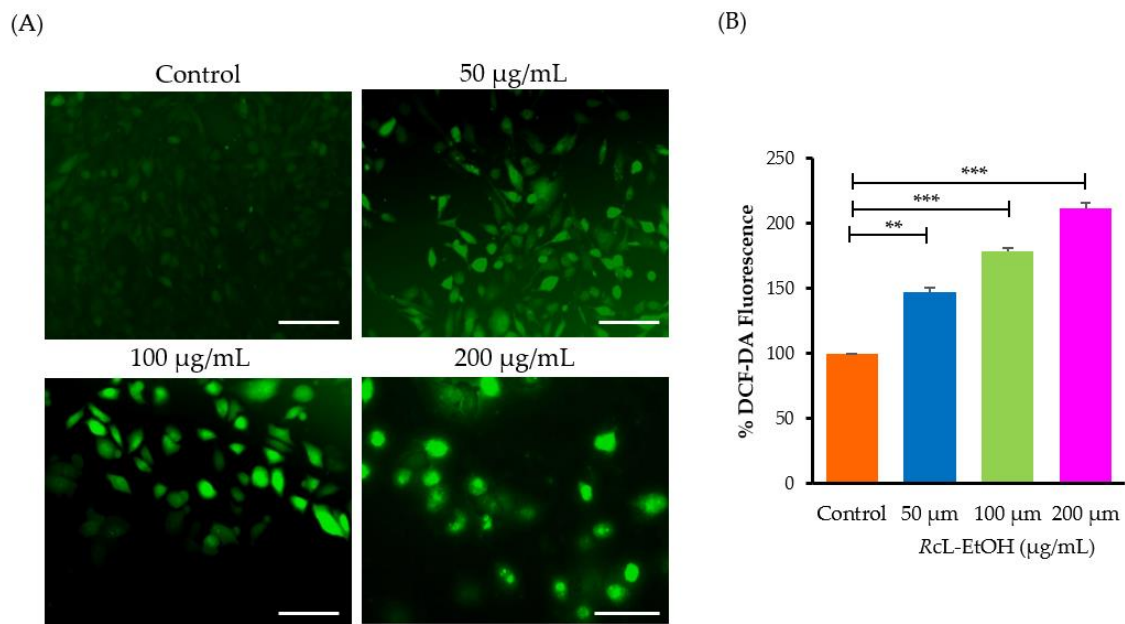


Figure 5. (A) Photomicrographs elucidating augmented ROS levels within A549 cells post-treatment with different concentrations of RcL-EtOH and subsequent staining with DCFH-DA. Scale bar = 100 µm. (B) Quantitative evaluation of fluorescence intensity. ** $p < 0.01$, *** $p < 0.001$ vs. control.

3.6. RcL-EtOH Modulated Expression of Apoptotic and Cell Cycle-Related Genes

Deregulation of the cell cycle and apoptosis mechanisms in normal cells is a key determinant for the development and/or progression of cancer [28]. Consequently, in order to gain more insight onto the underlying mechanism of the anticancer activity of RcL-EtOH against A549 cells, the mRNA expression levels of cell cycle- and apoptosis-regulating genes were assessed using a qRT-PCR analysis. As shown in Figure 6, the mRNA expression levels of anti-apoptotic markers; namely, Bcl-2 and Bcl_{XL}, were remarkably downregulated in RcL-EtOH-treated cells. The mRNA expression of Bcl-2 was decreased to 0.88 ± 0.03 , 0.71 ± 0.05 and 0.55 ± 0.03 -fold (Figure 6A), whereas that of Bcl_{XL} was observed to be reduced by 0.90 ± 0.03 , 0.78 ± 0.07 and 0.45 ± 0.02 -fold, compared to untreated cells (Figure 6B). By contrary, treatment with RcL-EtOH efficiently triggered a remarkable increase in the expression levels of pro-apoptotic markers; namely, Bax and Bad (Figure 6C,D). Of note, treatment with 200 µg/mL of RcL-EtOH resulted in a more than two-fold increase (2.16 ± 0.09 and 2.31 ± 0.08) in the expression of both tested pro-apoptotic genes (Bax and Bad), respectively. These findings suggest that RcL-EtOH-mediated apoptosis might be elicited via upregulating the expression of pro-apoptotic proteins, while down regulating the expression of anti-apoptotic proteins in A549 cells.

RcL-EtOH-mediated alteration of genes involved in cell cycle regulation and/or progression was further evaluated in A549 cells. RcL-EtOH reduced the mRNA expression of cyclinD1 and CDK4 within A549 cells in a dose-dependent manner (Figure 7). The alterations in the cyclinD1 expression were calculated to be 0.85 ± 0.03 fold (50 µg/mL); 0.57 ± 0.04 fold (100 µg/mL) and 0.35 ± 0.04 fold (200 µg/mL), in comparison with the control. Whereas, RcL-EtOH reduced CDK4 mRNA to 0.86 ± 0.04 fold (50 µg/mL); 0.56 ± 0.02 fold (100 µg/mL) and 0.25 ± 0.03 fold (200 µg/mL), when compared to the untreated A549 cells. On the other hand, treatment of A549 cells with RcL-EtOH remarkably augmented the expression of the cell cycle inhibitor p21^{Cip1} gene, the mRNA expression levels were 1.57 ± 0.07 -fold (50 µg/mL); 2.12 ± 0.10 -fold (100 µg/mL) and 2.33 ± 0.05 -fold (200 µg/mL), as compared with the untreated control (Figure 7). Our findings suggest that RcL-EtOH can cause cell cycle arrest by decreasing the expression levels of CDK4 and cyclin D1 genes while increasing the expression of the cell cycle inhibitor; p21^{Cip1} gene.

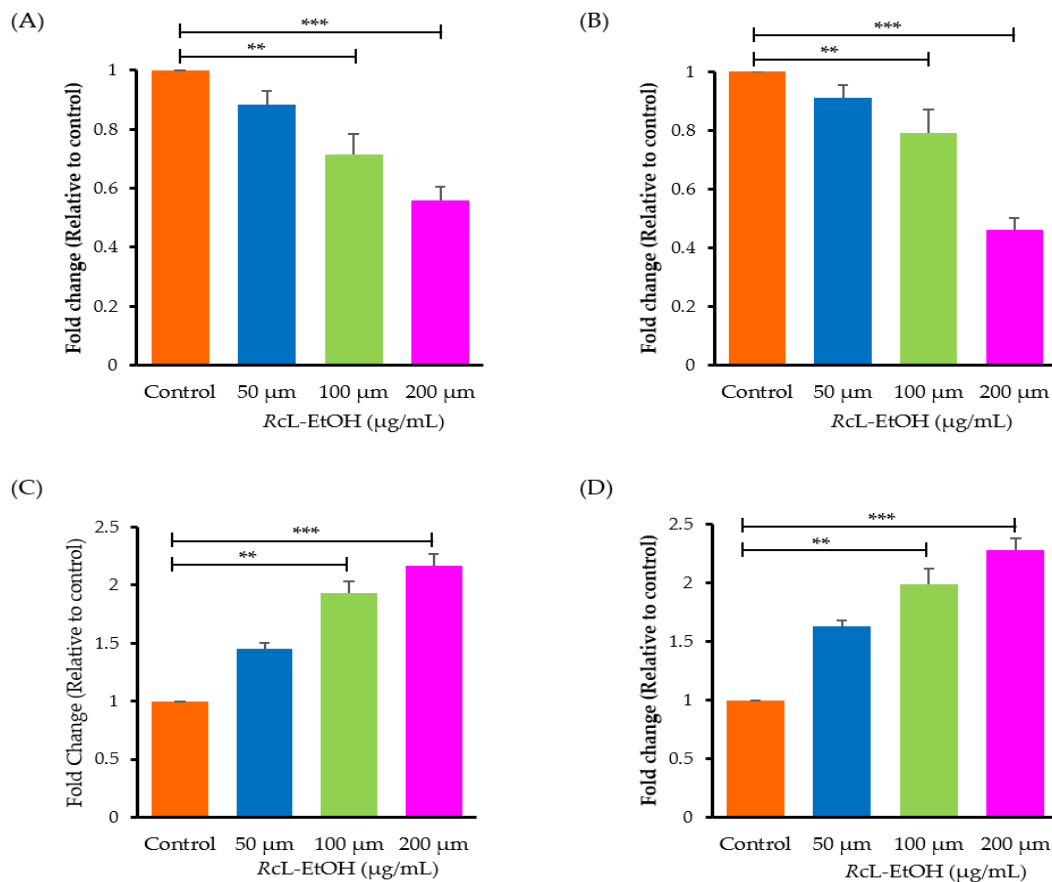


Figure 6. Changes within the mRNA expression of anti-apoptotic genes; (A) Bcl2; (B) Bcl_{XL} and pro-apoptotic genes; (C) Bax; (D) Bad. ** $p < 0.01$ and *** $p < 0.001$ vs. control.

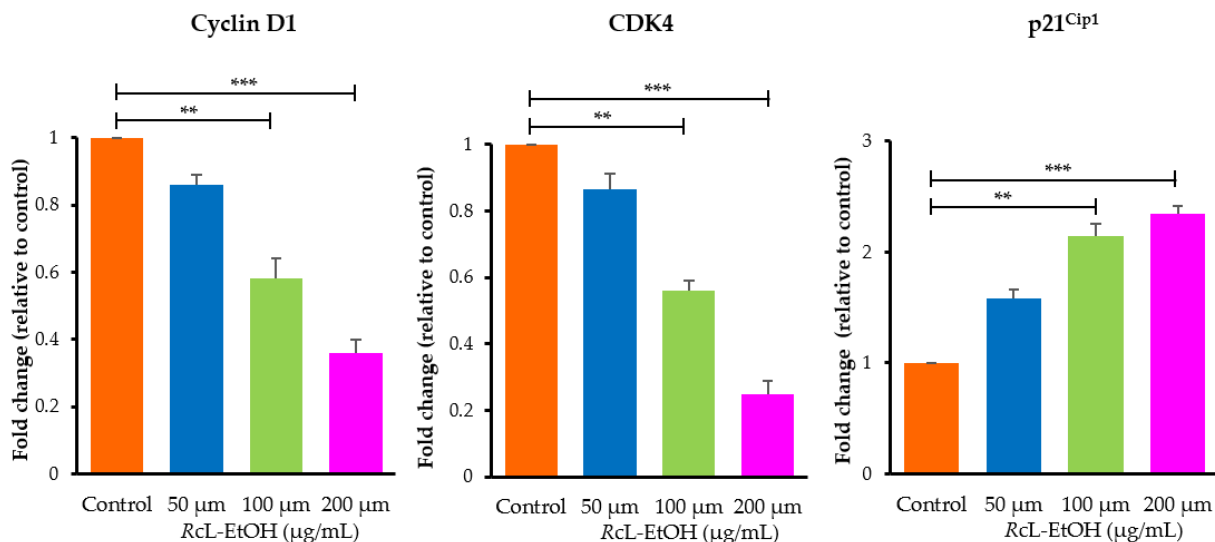


Figure 7. Changes within the mRNA expression of genes involved in cell cycle progression (cyclin D1, CDK4 and p21^{Cip1}) after exposure to RgL-EtOH. ** $p < 0.01$ and *** $p < 0.001$ vs. control.

4. Discussion

R. chingii is a traditional Chinese medicinal herbal that has been used since ancient times for its great dietary and medicinal values. Accumulating evidence revealed that *R. chingii* extracts possess diverse pharmacological actions, including anti-inflammatory, antibacterial, antioxidant, and anti-aging effects [11,12]. Most importantly, many reports

have underscored the potent cytotoxic effect of *R. chingii* extracts against a wide variety of cancer cells, including breast cancer, hepatic cancer, bladder cancer and lung cancer [14–16]. Nevertheless, the exact mechanism underlying the anticancer activity of *R. chingii* has not been fully elucidated. In this study, therefore, the cytotoxic potential of *R. chingii* ethanolic leaf extract (RcL-EtOH) against the non-small cell lung cancer (A549) cells was investigated. In addition, the probable mechanism underlying the anticancer activity of RcL-EtOH was addressed. RcL-EtOH efficiently suppressed A549 cell proliferation by inducing apoptosis, while having no significant inhibitory effects on normal murine alveolar macrophage J774A.1 cells. Intriguingly, the considerably lower cytotoxicity of RcL-EtOH against normal murine alveolar macrophage J774A.1 cells might be ascribed to the scarcity of oleoyl-CoA in RcL-EtOH. Generally, macrophage apoptosis is induced by free cholesterol-loading via C/EBP homologous protein (CHOP) pathway [29,30]. Low oleoyl-CoA can impede macrophage acetyl-CoA acetyltransferase (ACAT1) activity, which, in turn, would inhibit the CHOP pathway and avoid the macrophage apoptosis [30,31]. Consequently, J774A.1 cells can survive the treatment of RcL-EtOH, which might represent an effective anticancer drug candidate with low toxicity to normal cells.

Cell death is a prerequisite for maintaining normal homeostasis and may occur either through apoptosis, autophagy, or necrosis [32]. The targeting of such cell death pathways has evolved as viable means for cancer therapeutics. Among the above-stated pathways, instigation of apoptosis is regarded as a potential therapeutic target for clinical management of various carcinomas. Apoptosis is characterized by DNA fragmentation and chromatin condensation, which were found in A549 cells following RcL-EtOH therapy. In addition, the results of dual acridine orange/ethidium bromide (AO/EB) fluorescence staining explicitly demonstrated the instigation of apoptotic pathways post-RcL-EtOH exposure. Furthermore, quantification of cells undergoing apoptosis revealed the competence of RcL-EtOH in instigating considerable apoptosis in a dose-dependent manner.

Generally, programmed cell death can be driven by the activation of two distinct molecular pathways; a mitochondrial-dependent intrinsic pathway and a death receptor-dependent extrinsic pathway [33]. Both pathways lead to the hierarchical activation of a family of cysteine proteases called caspases. Herein, the treatment with RcL-EtOH has resulted in a significant dissipation of $\Delta\Psi_m$ as evidenced by the dose-dependent drop in Rh 123 dye uptake by A549 cells, as compared to untreated cells. Most importantly, RcL-EtOH-mediated alteration in $\Delta\Psi_m$ was accompanied with an elevated levels of cytosolic cytochrome c, which efficiently triggered caspase cascade activation within A549 cells. Intriguingly, it was observed that RcL-EtOH-mediated cytotoxicity was partially ameliorated in A549 cells that were pretreated with specific caspase inhibitors. These results suggest that RcL-EtOH-mediated apoptosis in non-small cell lung cancer A549 cells involves the loss of $\Delta\Psi_m$, release of mitochondrial cytochrome c, and activation of the caspase cascade, which are collectively related to the intrinsic mitochondrial-mediated cell death pathway. Similar findings were revealed by Gharbaran et al. [34], who reported that plumbagin, an active compound found in the root of *Plumbago zeylanica* plant, could exert a potent cytotoxic effect against metastatic retinoblastoma cells via disrupting $\Delta\Psi_m$ with a subsequent activation of the caspase cascade.

ROS in cancer cells plays a vital role in regulating cell death. Recent reports have highlighted the critical role of ROS in the anticancer actions of natural products, particularly phytochemicals [17,35]. In addition, it is well recognized that the production of ROS is one of the possible events triggered by the loss of mitochondrial integrity [36,37]. Consequently, in this study, we scrutinized the contribution of ROS production to the cytotoxic effect of RcL-EtOH against A549 cells. Treatment of A549 cells with RcL-EtOH resulted in a dose-dependent instigation of intracellular ROS levels within A549 cells. Most importantly, the cytotoxic potential of RcL-EtOH was remarkably blocked in A549 pretreated with N-acetylcysteine (NAC). NAC is a thiol compound that boosts glutathione levels [38], and it is considered one of the efficient ROS scavengers that can protect cells from the effect of elevated intracellular ROS levels. These findings suggested that the RcL-EtOH-induced

cytotoxic effect in A549 cells is mediated, at least in part, by ROS generation. Similar to our findings, recent studies have reported a ROS-mediated cell death in A549 cells induced by compounds isolated from natural products [20,39,40].

Abrogating the progression of cell cycle is an effective strategy in formulating effective chemotherapeutics for different cancers [41]. Generally, the regulation of cell cycle is under the strict activation and/or deactivation of cyclins and their associated kinases (CDKs) and their functional inactivation leads to cell cycle arrest [42]. In the current study, we verified the impeding effects of R_cL-EtOH on the mRNA expression of cyclinD1 and CDK4, along with the augmenting effect on the mRNA expression of the cell cycle inhibitor p21^{Cip1}, which might be linked to the efficacy of R_cL-EtOH in obstructing cell cycle progression, and thereby, inhibiting the proliferation of A549 cells. Collectively, our results suggested that the R_cL-EtOH-instigated apoptotic cell death within A549 cells was accomplished via a concomitant increase in ROS generation, dissipation of $\Delta\Psi_m$ followed by caspase activation, and altering the expression of gene regulating apoptosis. Nevertheless, further studies are needed to fully elucidate the molecular pathway(s) of R_cL-EtOH-mediated apoptosis in human A549 lung cancer cells.

There are some limitations of the present study. The lack of cell-cycle analysis limits determining whether the *R. chingii* extract elicits cell-cycle arrest, and thereby, could contribute to the cytotoxic mechanism(s) of action. In addition, the qualitative evaluation of the expression level of caspase-3/9 and gene(s) involved in cell cycle regulation and/or progression such as (cyclin D1, CDK4 and p21^{Cip1}) by Western blotting was not carried out. Moreover, in-depth analysis of phytochemical composition of the ethanolic extract of *R. chingii* leaves is urgently needed to exactly elucidate the active phyto-constituents in the leaves of *R. chingii* responsible for the observed promising cytotoxic activity against A549 lung cancer cells. Nevertheless, despite these limitations, the findings of our study clearly underscored the significance of the *R. chingii* leaf extract as a potential therapeutic option for the management of lung cancer.

5. Conclusions

In this study, we demonstrated that R_cL-EtOH could represent an effective anti-cancer candidate owing to its anti-proliferative efficacy and its competence of inducing apoptosis within A549 cells. The anticancer effect of R_cL-EtOH was manifested through the induction of mitochondria-mediated intrinsic apoptosis triggered by reactive oxygen species (ROS), as evidenced by dissipation of $\Delta\Psi_m$, bax/bcl-2 dysregulation, and activation of caspases 3 and 9. Collectively, R_cL-EtOH might represent a plausible therapeutic option for the management of lung cancer. Nevertheless, further exhaustive in vivo studies are a prerequisite for completely establishing the efficacy of R_cL-EtOH against non-small cell lung cancer.

Supplementary Materials: The following supporting information can be downloaded at: <https://www.mdpi.com/article/10.3390/pr10081537/s1>, Figure S1: The cytotoxic potential of R_cL-EtOH against A549 upon pretreatment with ROS inhibitor; N-acetyl-L-cysteine (NAC).

Author Contributions: Conceptualization, A.S.A.L. and E.-S.K.; methodology, A.S.A.L., A.A.S., H.F.A. and E.-S.K.; software, A.S.A.L.; formal analysis, A.A.S., H.F.A. and E.-S.K.; investigation, A.S.A.L., A.A.S., H.F.A. and E.-S.K.; resources, A.A.S. and H.F.A.; data curation, A.S.A.L.; writing—original draft preparation, A.S.A.L. and E.-S.K.; writing—review and editing, A.S.A.L.; funding acquisition, H.F.A. All authors have read and agreed to the published version of the manuscript.

Funding: This work was supported by the Princess Nourah bint Abdulrahman University researchers supporting project number (PNURSP2022R205), Princess Nourah bint Abdulrahman University, Riyadh, Saudi Arabia.

Institutional Review Board Statement: Not applicable.

Informed Consent Statement: Not applicable.

Data Availability Statement: All data can be found within this article and its supplementary information.

Acknowledgments: The authors extend their appreciation to Princess Nourah bint Abdulrahman University, Riyadh, Saudi Arabia for supporting this work under the researcher supporting project number (PNURSP2022R205).

Conflicts of Interest: The authors declare no conflict of interest.

References

1. World Health Organization Factsheet on Cancer. Available online: <https://www.who.int/news-room/fact-sheets/detail/cancer> (accessed on 15 April 2022).
2. Global Cancer Observatory Fact Sheet on Lung Cancer. Available online: <https://gco.iarc.fr/today/data/factsheets/cancers/15-Lung-fact-sheet.pdf> (accessed on 15 April 2022).
3. Molina, J.R.; Yang, P.; Cassivi, S.D.; Schild, S.E.; Adjei, A.A. Non-small cell lung cancer: Epidemiology, risk factors, treatment, and survivorship. *Mayo Clin. Proc.* **2008**, *83*, 584–594. [[CrossRef](#)]
4. Zappa, C.; Mousa, S.A. Non-small cell lung cancer: Current treatment and future advances. *Transl. Lung Cancer Res.* **2016**, *5*, 288–300. [[CrossRef](#)]
5. Zhang, M.; Li, M.; Du, L.; Zeng, J.; Yao, T.; Jin, Y. Paclitaxel-in-liposome-in-bacteria for inhalation treatment of primary lung cancer. *Int. J. Pharm.* **2020**, *578*, 119177. [[CrossRef](#)]
6. Lynch, T.J., Jr.; Kass, F.; Kalish, L.A.; Elias, A.D.; Strauss, G.; Shulman, L.N.; Sugarbaker, D.J.; Skarin, A.; Frei, E., 3rd. Cisplatin, 5-fluorouracil, and etoposide for advanced non-small cell lung cancer. *Cancer* **1993**, *71*, 2953–2957. [[CrossRef](#)]
7. Li, N.; Mai, Y.; Liu, Q.; Gou, G.; Yang, J. Docetaxel-loaded D- α -tocopheryl polyethylene glycol-1000 succinate liposomes improve lung cancer chemotherapy and reverse multidrug resistance. *Drug Deliv. Transl. Res.* **2021**, *11*, 131–141. [[CrossRef](#)] [[PubMed](#)]
8. Atanasov, A.G.; Waltenberger, B.; Pferschy-Wenzig, E.-M.; Linder, T.; Wawrosch, C.; Uhrin, P.; Temml, V.; Wang, L.; Schwaiger, S.; Heiss, E.H.; et al. Discovery and resupply of pharmacologically active plant-derived natural products: A review. *Biotechnol. Adv.* **2015**, *33*, 1582–1614. [[CrossRef](#)] [[PubMed](#)]
9. Vaou, N.; Stavropoulou, E.; Voidarou, C.; Tsigalou, C.; Bezirtzoglou, E. Towards Advances in Medicinal Plant Antimicrobial Activity: A Review Study on Challenges and Future Perspectives. *Microorganisms* **2021**, *9*, 2041. [[CrossRef](#)]
10. Wang, H.; Khor, T.O.; Shu, L.; Su, Z.-Y.; Fuentes, F.; Lee, J.-H.; Kong, A.-N.T. Plants vs. cancer: A review on natural phytochemicals in preventing and treating cancers and their druggability. *Anticancer Agents Med. Chem.* **2012**, *12*, 1281–1305. [[CrossRef](#)]
11. Yu, G.; Luo, Z.; Wang, W.; Li, Y.; Zhou, Y.; Shi, Y. *Rubus chingii* Hu: A Review of the Phytochemistry and Pharmacology. *Front. Pharmacol.* **2019**, *10*, 799. [[CrossRef](#)]
12. Ding, H.-Y. Extracts and Constituents of *Rubus chingii* with 1,1-Diphenyl-2-picrylhydrazyl (DPPH) Free Radical Scavenging Activity. *Int. J. Mol. Sci.* **2011**, *12*, 3941–3949. [[CrossRef](#)]
13. Li, K.; Zeng, M.; Li, Q.; Zhou, B. Identification of polyphenolic composition in the fruits of *Rubus chingii* Hu and its antioxidant and antiproliferative activity on human bladder cancer T24 cells. *J. Food Meas. Charact.* **2019**, *13*, 51–60. [[CrossRef](#)]
14. Zhang, T.T.; Lu, C.L.; Jiang, J.G.; Wang, M.; Wang, D.M.; Zhu, W. Bioactivities and extraction optimization of crude polysaccharides from the fruits and leaves of *Rubus chingii* Hu. *Carbohydr. Polym.* **2015**, *130*, 307–315. [[CrossRef](#)] [[PubMed](#)]
15. Zhang, T.T.; Yang, L.; Jiang, J.G. Bioactive comparison of main components from unripe fruits of *Rubus chingii* Hu and identification of the effective component. *Food Funct.* **2015**, *6*, 2205–2214. [[CrossRef](#)]
16. Zhang, T.-T.; Liu, Y.-J.; Yang, L.; Jiang, J.-G.; Zhao, J.-W.; Zhu, W. Extraction of antioxidant and antiproliferative ingredients from fruits of *Rubus chingii* Hu by active tracking guidance. *MedChemComm* **2017**, *8*, 1673–1680. [[CrossRef](#)]
17. Al Saqr, A.; Khafagy, E.S.; Aldawsari, M.F.; Almansour, K.; Abu Lila, A.S. Screening of Apoptosis Pathway-Mediated Anti-Proliferative Activity of the Phytochemical Compound Furanodienone against Human Non-Small Lung Cancer A-549 Cells. *Life* **2022**, *12*, 114. [[CrossRef](#)] [[PubMed](#)]
18. Rastogi, R.P.; Singh, S.P.; Häder, D.P.; Sinha, R.P. Detection of reactive oxygen species (ROS) by the oxidant-sensing probe 2',7'-dichlorodihydrofluorescein diacetate in the cyanobacterium *Anabaena variabilis* PCC 7937. *Biochem. Biophys. Res. Commun.* **2010**, *397*, 603–607. [[CrossRef](#)] [[PubMed](#)]
19. Mishra, T.; Arya, R.K.; Meena, S.; Joshi, P.; Pal, M.; Meena, B.; Upreti, D.K.; Rana, T.S.; Datta, D. Isolation, Characterization and Anticancer Potential of Cytotoxic Triterpenes from *Betula utilis* Bark. *PLoS ONE* **2016**, *11*, e0159430. [[CrossRef](#)] [[PubMed](#)]
20. Ahmad, A.; Tiwari, R.K.; Almeleebia, T.M.; Al Fayi, M.S.; Alshahrani, M.Y.; Ahmad, I.; Abohassan, M.S.; Saeed, M.; Ansari, I.A. *Swertia chirayita* suppresses the growth of non-small cell lung cancer A549 cells and concomitantly induces apoptosis via downregulation of JAK1/STAT3 pathway. *Saudi J. Biol. Sci.* **2021**, *28*, 6279–6288. [[CrossRef](#)]
21. Liu, K.; Liu, P.C.; Liu, R.; Wu, X. Dual AO/EB staining to detect apoptosis in osteosarcoma cells compared with flow cytometry. *Med. Sci. Monit. Basic Res.* **2015**, *21*, 15. [[CrossRef](#)]
22. Zorova, L.D.; Popkov, V.A.; Plotnikov, E.Y.; Silachev, D.N.; Pevzner, I.B.; Jankauskas, S.S.; Babenko, V.A.; Zorov, S.D.; Balakireva, A.V.; Juhaszova, M.; et al. Mitochondrial membrane potential. *Anal. Biochem.* **2018**, *552*, 50–59. [[CrossRef](#)]

23. Castera, L.; Hatzfeld-Charbonnier, A.S.; Ballot, C.; Charbonnel, F.; Dhuiege, E.; Velu, T.; Formstecher, P.; Mortier, L.; Marchetti, P. Apoptosis-related mitochondrial dysfunction defines human monocyte-derived dendritic cells with impaired immuno-stimulatory capacities. *J. Cell. Mol. Med.* **2009**, *13*, 1321–1335. [[CrossRef](#)] [[PubMed](#)]
24. Borutaite, V.; Budriunaite, A.; Morkuniene, R.; Brown, G.C. Release of mitochondrial cytochrome c and activation of cytosolic caspases induced by myocardial ischaemia. *Biochim. Et Biophys. Acta (BBA)—Mol. Basis Dis.* **2001**, *1537*, 101–109. [[CrossRef](#)]
25. Elena-Real, C.A.; Díaz-Quintana, A.; González-Arzola, K.; Velázquez-Campoy, A.; Orzáez, M.; López-Rivas, A.; Gil-Caballero, S.; De la Rosa, M.Á.; Díaz-Moreno, I. Cytochrome c speeds up caspase cascade activation by blocking 14-3-3 ϵ -dependent Apaf-1 inhibition. *Cell Death Dis.* **2018**, *9*, 365. [[CrossRef](#)] [[PubMed](#)]
26. Logue, S.E.; Martin, S.J. Caspase activation cascades in apoptosis. *Biochem. Soc. Trans.* **2008**, *36*, 1–9. [[CrossRef](#)]
27. Aggarwal, V.; Tuli, H.S.; Varol, A.; Thakral, F.; Yerer, M.B.; Sak, K.; Varol, M.; Jain, A.; Khan, M.A.; Sethi, G. Role of Reactive Oxygen Species in Cancer Progression: Molecular Mechanisms and Recent Advancements. *Biomolecules* **2019**, *9*, 735. [[CrossRef](#)]
28. Pistrutto, G.; Trisciuglio, D.; Ceci, C.; Garufi, A.; D'Orazi, G. Apoptosis as anticancer mechanism: Function and dysfunction of its modulators and targeted therapeutic strategies. *Aging (Albany NY)* **2016**, *8*, 603–619. [[CrossRef](#)]
29. Tsukano, H.; Gotoh, T.; Endo, M.; Miyata, K.; Tazume, H.; Kadomatsu, T.; Yano, M.; Iwawaki, T.; Kohno, K.; Araki, K.; et al. The Endoplasmic Reticulum Stress-C/EBP Homologous Protein Pathway-Mediated Apoptosis in Macrophages Contributes to the Instability of Atherosclerotic Plaques. *Arterioscler. Thromb. Biol.* **2010**, *30*, 1925–1932. [[CrossRef](#)]
30. Hu, H.; Tian, M.; Ding, C.; Yu, S. The C/EBP Homologous Protein (CHOP) Transcription Factor Functions in Endoplasmic Reticulum Stress-Induced Apoptosis and Microbial Infection. *Front. Immunol.* **2019**, *9*, 3083. [[CrossRef](#)]
31. Hai, Q.; Smith, J.D. Acyl-Coenzyme A: Cholesterol Acyltransferase (ACAT) in Cholesterol Metabolism: From Its Discovery to Clinical Trials and the Genomics Era. *Metabolites* **2021**, *11*, 543. [[CrossRef](#)]
32. Nikolettou, V.; Markaki, M.; Palikaras, K.; Tavernarakis, N. Crosstalk between apoptosis, necrosis and autophagy. *Biochim Biophys Acta* **2013**, *1833*, 3448–3459. [[CrossRef](#)]
33. Elmore, S. Apoptosis: A review of programmed cell death. *Toxicol. Pathol.* **2007**, *35*, 495–516. [[CrossRef](#)] [[PubMed](#)]
34. Gharbaran, R.; Shi, C.; Onwumere, O.; Redenti, S. Plumbagin Induces Cytotoxicity via Loss of Mitochondrial Membrane Potential and Caspase Activation in Metastatic Retinoblastoma. *Anticancer Res.* **2021**, *41*, 4725–4732. [[CrossRef](#)] [[PubMed](#)]
35. Khan, A.Q.; Rashid, K.; AlAmodi, A.A.; Agha, M.V.; Akhtar, S.; Hakeem, I.; Raza, S.S.; Uddin, S. Reactive oxygen species (ROS) in cancer pathogenesis and therapy: An update on the role of ROS in anticancer action of benzophenanthridine alkaloids. *Biomed. Pharmacother.* **2021**, *143*, 112142. [[CrossRef](#)]
36. Marchi, S.; Giorgi, C.; Suski, J.M.; Agnoletto, C.; Bononi, A.; Bonora, M.; De Marchi, E.; Missiroli, S.; Patergnani, S.; Poletti, F.; et al. Mitochondria-Ros Crosstalk in the Control of Cell Death and Aging. *J. Signal Transduct.* **2012**, *2012*, 329635. [[CrossRef](#)] [[PubMed](#)]
37. Zorov, D.B.; Juhaszova, M.; Sollott, S.J. Mitochondrial reactive oxygen species (ROS) and ROS-induced ROS release. *Physiol. Rev.* **2014**, *94*, 909–950. [[CrossRef](#)]
38. Pedre, B.; Barayeu, U.; Ezeriņa, D.; Dick, T.P. The mechanism of action of N-acetylcysteine (NAC): The emerging role of H₂S and sulfane sulfur species. *Pharmacol. Ther.* **2021**, *228*, 107916. [[CrossRef](#)]
39. Lin, X.M.; Liu, S.B.; Luo, Y.H.; Xu, W.T.; Zhang, Y.; Zhang, T.; Xue, H.; Zuo, W.B.; Li, Y.N.; Lu, B.X.; et al. 10-HDA Induces ROS-Mediated Apoptosis in A549 Human Lung Cancer Cells by Regulating the MAPK, STAT3, NF- κ B, and TGF- β 1 Signaling Pathways. *Biomed Res. Int.* **2020**, *2020*, 3042636. [[CrossRef](#)]
40. Zhang, G.Y.; Chen, W.Y.; Li, X.B.; Ke, H.; Zhou, X.L. Scutellarin-induced A549 cell apoptosis depends on activation of the transforming growth factor- β 1/smad2/ROS/caspase-3 pathway. *Open Life Sci.* **2021**, *16*, 961–968. [[CrossRef](#)]
41. Al Saqr, A.; Wani, S.U.D.; Gangadharappa, H.V.; Aldawsari, M.F.; Khafagy, E.-S.; Lila, A.S.A. Enhanced Cytotoxic Activity of Docetaxel-Loaded Silk Fibroin Nanoparticles against Breast Cancer Cells. *Polymers* **2021**, *13*, 1416. [[CrossRef](#)]
42. Ding, L.; Cao, J.; Lin, W.; Chen, H.; Xiong, X.; Ao, H.; Yu, M.; Lin, J.; Cui, Q. The Roles of Cyclin-Dependent Kinases in Cell-Cycle Progression and Therapeutic Strategies in Human Breast Cancer. *Int. J. Mol. Sci.* **2020**, *21*, 1960. [[CrossRef](#)]